ORGANOMETALLICS

pubs.acs.org/Organometallics Article

Platinum ω-Alkenyl Compounds as Chemical Vapor Deposition Precursors. Mechanistic Studies of the Thermolysis of $Pt[CH_2CMe_2CH_2CH{=}CH_2]_2$ in Solution and the Origin of Rapid Nucleation

Sumeng Liu, Zhejun Zhang, John R. Abelson, and Gregory S. Girolami*

Cite This: *Organometallics* 2020, 39, 3817–3829 Read Online

ACCESS | Metrics & More | Article Recommendations | Supporting Information

ABSTRACT: The compound *cis*-bis(η^1,η^2-2,2-dimethylpent-4-en-1-yl)platinum, $Pt[CH_2CMe_2CH_2CH{=}CH_2]_2$ (**3**), is a recently discovered chemical vapor deposition (CVD) precursor for the deposition of highly smooth platinum thin films without nucleation delays on a variety of substrates. This paper describes detailed mechanistic studies of the pathway by which **3** reacts upon being heated in solution. In various solvents between 90 and 130 °C, **3** decomposes to generate ∼1 equiv of 4,4-dimethylpentenes by addition of a hydrogen atom to the pentenyl ligands in **3**. The "extra" hydrogen atoms arise by dehydrogenation of other pentenyl ligands; some of these dehydrogenated ligands are released as methyl-substituted methylenecyclobutanes and cyclobutenes. A combination of isotope labeling and kinetic studies suggests that **3** decomposes by C−H activation of both allylic and olefinic C−H bonds to give transient platinum hydride intermediates, followed by reductive elimination steps to form the pentene products, but that the exact mechanism is solvent-dependent. In C_6F_6, solvent association occurs before C−H bond activation, and the rate-determining step for thermolysis is most likely the formation of a Pt σ complex. In hydrocarbon solvents, the solvent is little involved before C−H bond activation, and the rate-determining step is most likely the formation of a Pt σ complex only for γ-C−H and ε-C−H bond activation, but cleavage or formation of a C−H bond for δ-C−H bond activation. A comparison of the thermolysis reactions under CVD conditions and in solution suggests that the high smoothness of the CVD-grown films is due in part to rapid nucleation (which is a consequence of the availability of low-barrier C=C bond dissociation pathways) and in part to the formation of carbon-containing species that passivate the Pt surface.

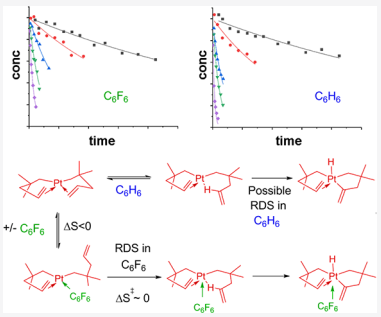

INTRODUCTION

The chemical vapor deposition (CVD)[1−5] and atomic layer deposition (ALD)[6−9] of platinum thin films from organoplatinum precursors is of interest for a wide variety of applications: as a gate electrode material,[10] as a diffusion barrier or ohmic contact in microelectronic structures,[11,12] as a catalyst,[13−16] as a component of data storage media,[17] and as an electrical contact in medical devices.[18−20] However, the deposition of platinum thin films from ALD or CVD generally suffers from poor nucleation[11,21−24] due to the differences in the reactivities[25] and surface energies[26] of common substrates and platinum. For example, the popular CVD and ALD precursor $(C_5H_4Me)PtMe_3$ has a high barrier to eliminate ligands when it is adsorbed on oxide surfaces[24,27] but reacts readily on Pt nuclei owing to the highly catalytic nature of platinum.[11,25,28] As a result of poor nucleation, the consequent island growth behavior makes it difficult to grow continuous films that are also very thin.

To solve this problem, one must increase the rate of nucleation on a relatively inert substrate surface (k_{sub}) vs that on catalytic platinum surfaces (k_{Pt}). Several approaches, such as using an oxygen plasma as a co-reactant[28] or employing a precursor whose ligands can be more easily eliminated,[29] have been used to enhance the reactivity of precursor molecules on substrates vs that on Pt nuclei. However, in both cases, a short nucleation delay persists.

In a separate paper,[30] we described the synthesis and characterization of *cis*-bis(η^1,η^2-2,2-dimethylpent-4-en-1-yl)-platinum, $Pt[CH_2CMe_2CH_2CH{=}CH_2]_2$ (**3**). Compound **3**, a liquid precursor with a relatively high vapor pressure (250 mTorr at 80 °C), can be stored at room temperature for months in air. In addition, **3** deposits very smooth platinum films without nucleation delays on several different substrates (SiO_2/Si, Al_2O_3, and VN). Qualitatively, **3** gives much smoother films than the commonly used methylcyclopenta-

Received: August 14, 2020
Published: October 26, 2020

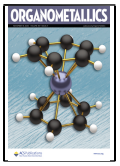

https://dx.doi.org/10.1021/acs.organomet.0c00542
Organometallics 2020, 39, 3817−3829

dienyl precursor $(C_5H_4Me)PtMe_3$, which we attribute to a combination of a low barrier for formation of reactive intermediates (which leads to fast generation of nuclei on low-reactivity substrates) and passivation of the growing platinum surface by dehydrogenation of the 2,2-dimethylpent-4-en-1-yl ligand (which reduces the rate of precursor decomposition on Pt nuclei).[30] A combination of both effects leads to a significant enhancement in the ratio k_{sub}/k_{Pt}, which leads to smoother films.

In the current paper, we describe studies to determine the mechanism and the kinetics by which **3** thermolyzes in solution. These studies also afford important insights into the origin of fast nucleation seen during CVD from **3** and the relationship between the structure of the precursor and the morphology of the resulting films.

RESULTS AND DISCUSSION

Possible Unimolecular Decomposition Mechanisms for 3. The thermolysis of $Pt[CH_2CMe_2CH_2CH{=}CH_2]_2$ (**3**) in solution could be initiated by several different mechanisms (Scheme 1), including (a) activation of one of the five different kinds of C−H bonds,[31−33] (b) migratory insertion of the C=C bond into the Pt−alkyl bond to form a (3,3-dimethylcyclobutyl)methyl group,[34,35] which subsequently undergoes β-hydrogen elimination, (c) β-alkyl or β-allyl elimination,[36−39] and (d) reductive elimination by C−C coupling of two pentenyl ligands.[40]

Scheme 1. Possible Decomposition Mechanisms of 3

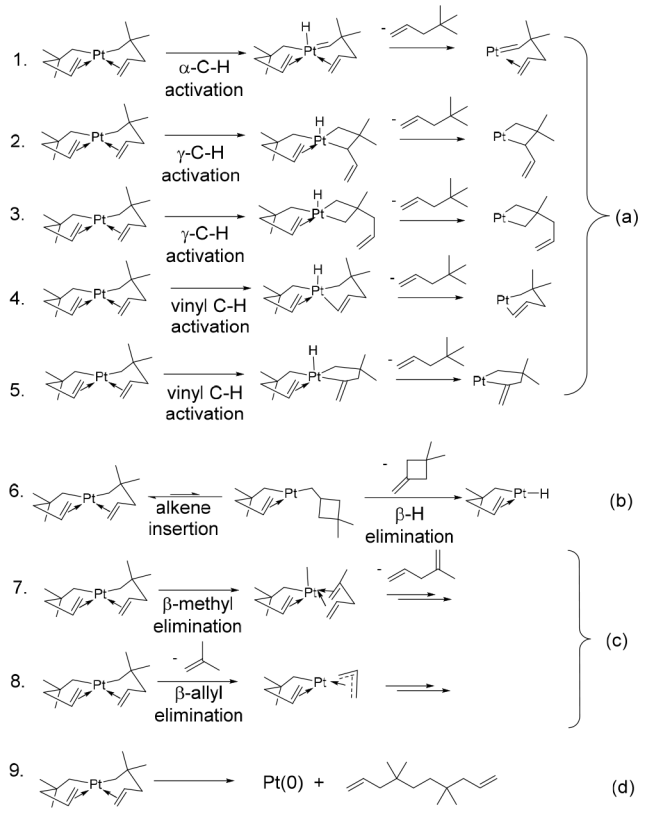

Many of these processes can be distinguished by analyzing the organic thermolysis byproducts.[41,42] For example, reductive elimination should generate 14-carbon species, whereas the β-methyl and β-allyl elimination pathways should result in the formation of hydrocarbons having fewer than 7 carbon atoms; in contrast, the other pathways should afford 7-carbon species.

Organic Products and Stoichiometry of Thermolysis of 3 in Different Solvents. In order to obtain information about the thermal reactivity of **3**, we carried out parallel thermolysis studies in sealed NMR tubes in four different solvents: hexafluorobenzene (C_6F_6), benzene (C_6H_6), deuterobenzene (C_6D_6), and deuterocyclohexane (C_6D_{12}). The room-temperature ^1H NMR spectra confirm that the structure of **3** seen in the solid state is maintained in all of these solvents.[30] In all of our thermolysis studies, the initial concentration of **3** was ~0.05−0.2 M, and a drop of mercury was added to inhibit secondary surface reactions on any colloidal platinum that formed.[43] In all four solvents, the thermolysis rates become significant only above about 90 °C.

Thermolyses conducted between 90 and 130 °C in the fluorocarbon C_6F_6 generate light yellow solutions and a black precipitate. Over the first ~1.5 half-lives, the principal organic products are 4,4-dimethyl-1-pentene and 4,4-dimethyl-2-pentene; these products are generated by adding one hydrogen atom to the 2,2-dimethylpentenyl ligands in **3** (Scheme 2).

Scheme 2. Products Generated upon Thermolysis of 3 in C_6F_6

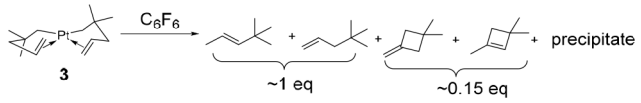

The 1- and 2-pentene isomers, which are present in a ratio of ~1:7, together constitute ~1 equiv per mole of **3** (Figure S3.1). Most likely, the 1-pentene isomer is formed initially, but over the long residence times in the NMR tube, it isomerizes in the presence of platinum to the thermodynamically more stable 2-pentene isomer.[44] The 7-carbon dehydrogenation products 1,1-dimethyl-3-methylenecyclobutane and its isomer 1,4,4-trimethylcyclobutene are also formed, but only in small amounts: about ~0.15 equiv total[45] is generated per mole of **3** (Figures S3.1−3.4).

C−F bond activation of the solvent is of negligible importance: during the first half-life no soluble fluorine-containing species other than C_6F_6 is present, and at longer times C_6F_5H can be detected but only in trace amounts (Figures S3.5 and 3.6).

Thermolyses conducted in the hydrocarbon solvents C_6H_6, C_6D_6, and C_6D_{12} generate brown solutions (indicative of the generation of colloidal Pt) and a black precipitate. When the thermolysis of **3** is conducted in C_6H_6 at 120 °C, the organic product distribution after ~2 half lives is very similar to that seen in C_6F_6 (Scheme 3). Specifically, the principal organic products are 4,4-dimethyl-1-pentene and 4,4-dimethyl-2-pentene (~1:10 ratio, together constituting ~1 equiv per mole of **3**; Figure S3.13). Also formed are small amounts (0.01

Scheme 3. Products Generated upon Thermolysis of 3 in Benzene at 120 °C

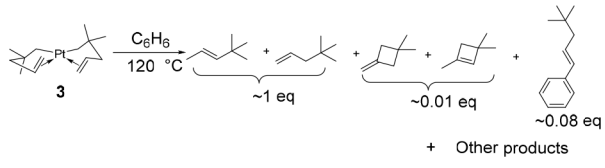

https://dx.doi.org/10.1021/acs.organomet.0c00542
Organometallics 2020, 39, 3817−3829

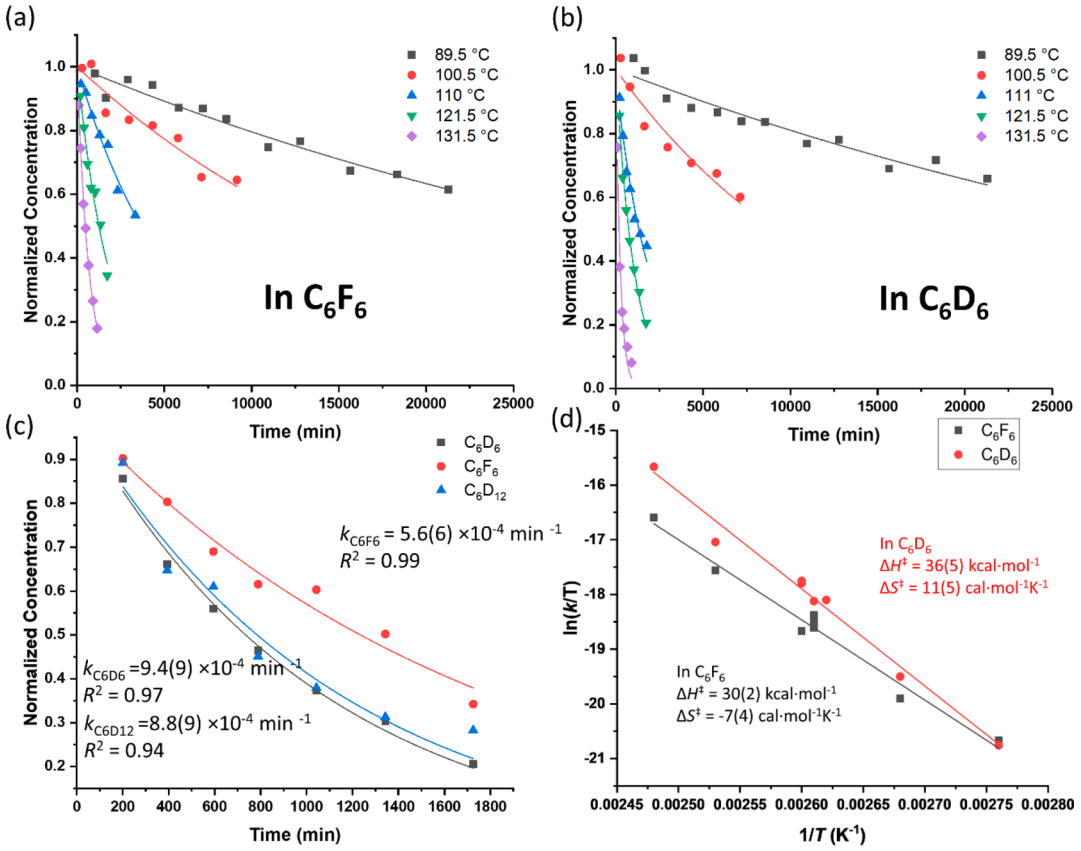

Figure 1. (a) Normalized concentration (i.e., $C_0 = 1$) of **3** vs time in C_6F_6 at different thermolysis temperatures, fit to $C = C_0e^{-kt}$. (b) Normalized concentration (i.e., $C_0 = 1$) of **3** vs time in C_6H_6 at different thermolysis temperatures, fit to $C = C_0e^{-kt}$. (c) Normalized concentration (i.e., $C_0 = 1$) vs time for the thermolysis of **3** at 121.5 °C in C_6F_6, C_6D_6, and C_6D_{12}. The integration was fit to $C = C_0e^{-kt}$. The rates of thermolysis in C_6D_6 and C_6D_{12} are similar, but slightly faster than that in C_6F_6. (d) Eyring plot for the thermolysis of **3** in C_6F_6 ($\Delta H^{\ddagger}_{obs}$ = 30(2) kcal mol^{-1} and $\Delta S^{\ddagger}_{obs}$ = −7(4) eu) vs Eyring plot for the thermolysis of **3** in C_6D_6 ($\Delta H^{\ddagger}_{obs}$ = 36(5) kcal mol^{-1} and $\Delta S^{\ddagger}_{obs}$ = 11(5) eu).

equiv total) of the 2,2-dimethylpentenyl dehydrogenation products 1,1-dimethyl-3-methylenecyclobutane and its isomer 1,4,4-trimethylcyclobutene; a small amount (~0.08 equiv) of the benzene activation product (*E*)-(4,4-dimethylpent-1-en-1-yl)benzene is also formed (Figures S3.12 and 3.13).

When the thermolysis of undeuterated **3** is carried out at 120 °C in C_6D_6, essentially no H−D exchange can be observed between unreacted **3** and solvent. Furthermore, only negligible amounts (~10%) of deuterium appear in the allylic and olefinic positions of the product pentenes, as observed in the ^{2}H NMR spectrum (Figure S3.14). Similarly small amounts (~10%) of deuterium also appear in the *tert*-butyl region, which we associate with the minor product (*E*)-(4,4-dimethylpent-1-en-1-yl)benzene; this species is probably formed by a secondary reaction in which C−D bonds of the deuterated solvent are activated after **3** decomposes (Scheme S3.1). All of these observations are consistent with the conclusion that C−H activation of the solvent is at best a very minor component of the pathway by which **3** thermolyzes.

When the thermolyses of **3** is conducted in C_6D_6 or C_6H_6 at lower temperatures, i.e., below 120 °C, a similar product distribution is seen, except that we see about 0.05 equiv of a new species, (*E*)-5-methylhexa-1,3-diene.[46] One possibility is that some of the directly formed thermolysis byproducts, such as this diene, are consumed or transformed over the course of the reaction owing to the present of catalytically active Pt species.

Because the thermolysis of **3** results in the formation of only trace amounts of light (<C_7) hydrocarbons and C_{14} species, we can rule out *β*-alkyl elimination, *β*-allyl elimination, and reductive coupling of the pentenyl groups as major decomposition pathways (mechanisms c and d, Scheme 1). Instead, thermolysis of **2** in solution most likely occurs by C−H bond activation of some of the 2,2-dimethylpentenyl groups (mechanism a, Scheme 1). The hydrogen atoms are transferred to other 2,2-dimethylpentenyl groups to generate the observed C_7 dimethylpentene products. Some of the dehydrogenated 2,2-dimethylpentenyl groups evidently undergo subsequent skeletal rearrangements and are released from Pt (in low yield) as methylenecyclobutanes or cyclobutenes.

Kinetics of the Thermolysis of Unlabeled 3 in Different Solvents. In C_6F_6, C_6H_6, C_6D_6, and C_6D_{12}, the thermolysis follows first-order kinetics over the first two half-lives (Figure 1 and Figures S3.7−S3.9 and S3.15−S3.17). At times longer than 2 half-lives, the thermolysis rate slows slightly in all four solvents relative to first-order kinetics.[47] In order to avoid complications arising from the deviation from first-order kinetics, the results discussed in the next several sections are derived from data collected during the first 2 half-lives.[48]

In all four solvents, the thermolysis of **3** obeys first-order kinetics, $d[3]/dt = -k_{obs}[3]$, over the first 2 half-lives. At 121.5 °C, the first-order rate constants of 9.4(9) × 10^{-4} min^{-1} in C_6D_6 and 8.8(9) × 10^{-4} min^{-1} in C_6D_{12} are equal within error (in a separate experiment, Figure S3.11, we found that the rate

https://dx.doi.org/10.1021/acs.organomet.0c00542
Organometallics 2020, 39, 3817−3829

constants in C_6D_6 and C_6H_6 are also identical within about 5%). In contrast, at 121.5 °C the first-order rate constant of $5.6(6) \times 10^{-4}$ min^{-1} in C_6F_6 is slightly but significantly slower (Figure 1). Thus, the rate constants in the three hydrocarbon solvents are all essentially identical but are about 60% larger than that in C_6F_6.

Fitting the rate of thermolysis between 90 and 130 °C to the Eyring equation gives the activation parameters $\Delta H^{\ddagger}$ = 36(5) kcal mol^{-1} and $\Delta S^{\ddagger}$ = 11(5) eu in C_6D_6 and $\Delta H^{\ddagger}$ = 30 (2) kcal mol^{-1} and $\Delta S^{\ddagger}$ = −7(4) eu in C_6F_6 (Figure 1). Particularly notable here is that the activation entropy is positive in C_6D_6 but negative in C_6F_6, with a difference of 18(6) eu. The different rate constants and activation parameters suggest that the mechanism by which **3** thermolyzes is different in C_6D_6 than in C_6F_6.

We can rule out the possibility that the faster thermolysis rate in the hydrocarbon solvents is due to reaction with the solvent: if solvent were reacting, then (1) the thermolysis rate constant should be different in benzene, deuterobenzene, and deuterocyclohexane, but in fact they are identical within experimental error and (2) the rate constant in C_6F_6 should increase if C_6H_6 is added, but in fact the addition of 1.4 equiv of benzene per mole of **3** gives a reaction rate and reaction byproducts that are the same as those when benzene is not added (see Figure S3.10). Furthermore, we showed above that C−H activation of benzene is negligible. We conclude that the main pathway for thermolysis of **3** in hydrocarbon solvents does not involve the direct participation of the solvent. In contrast, the slower rate of (and different activation parameters for) thermolysis of **3** in C_6F_6 may be due to a change in the reaction mechanism in this solvent. We will return to this point later.

Finally, we also observed that, in both C_6D_6 and C_6F_6, the rate constant for generation of the 4,4-dimethylpentene isomers (the major organic products) is essentially the same as the rate constant for thermolysis of **3** (Figures S3.25 and S3.26 and Table S3.1). In addition, no organoplatinum species other than **3** are ever observed in solution. We will discuss the mechanistic ramifications of these observations in a later section.

Isotope Labeling Studies: Identification of the C−H Bonds That Are Activated during Thermolysis. Five deuterium-labeled isotopologues of *cis*-bis(η^1,η^2-2,2-dimethylpent-4-en-1-yl)platinum were synthesized to study the C−H activation step: these are **3**-α-d_4, **3**-β-Me-d_{12}, **3**-γ-d_4, **3**-δ-d_2, and **3**-ε-d_4 (Scheme 4):

We showed above that, during thermolysis, the 4,4-dimethylpentene thermolysis products obtain their "extra" hydrogen atom from other pentenyl ligands in **3**. The extra hydrogen atom is added to the Pt-bound α-CH_2 group, which is thereby converted into a methyl group to form the 4,4-dimethylpentene products (which can also be viewed as *tert*-butyl-substituted propenes). The origin of the extra hydrogen atom can be identified by analyzing the deuterium content in the *tert*-butyl group of the 4,4-dimethylpentene thermolysis products generated from each of the five deuterated isotopologues of **3**.

For thermolyses of **3**-α-d_4 or **3**-β-Me-d_{12} conducted in C_6F_6 at 110 °C, quantitative ^1H and ^2H NMR analyses (see section 5 in the Supporting Information) show that, within experimental error, the 4,4-dimethylpentene products are formed exclusively by addition of one hydrogen atom to the pentenyl ligands; from the absence of any deuterium transfer, we can conclude that little activation of the α-CH_2 and β-Me positions occurs. In contrast, for thermolyses of **3**-γ-d_4, **3**-δ-d_2, and **3**-ε-d_4 under the same conditions, we find that the 4,4-dimethylpentene products are generated partially by addition of a deuterium atom and partially by addition of a hydrogen atom: on a mole fraction basis, 0.2(1), 0.27(5), and 0.33(8) are respectively formed by adding one D atom to the pentenyl ligands, and the rest are formed by adding one H atom (Scheme 5 and Table S5.1 and Figures S5.3, S5.14, and S5.20). This result suggests that, somewhat surprisingly, the γ-CH_2, δ-CH, and ε-CH_2 positions are all being activated.

Thermolysis of the deuterated isotopologues of **3** in C_6H_6 give similar but not identical results. The results of the thermolysis of **3**-γ-d_4, **3**-δ-d_2, and **3**-ε-d_4 show that all of these C−H bonds are activated: on a mole fraction basis, 0.5(1), 0.15(4), and 0.28(5), respectively, of the 4,4-dimethylpentenes

Scheme 4. Five Deuterated Isotopologues of 3 Used in This Study

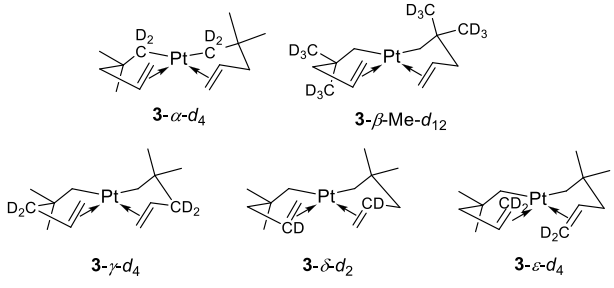

Scheme 5. Products from the Thermolysis of the Various Isotopologues of 3 in C_6F_6[a]

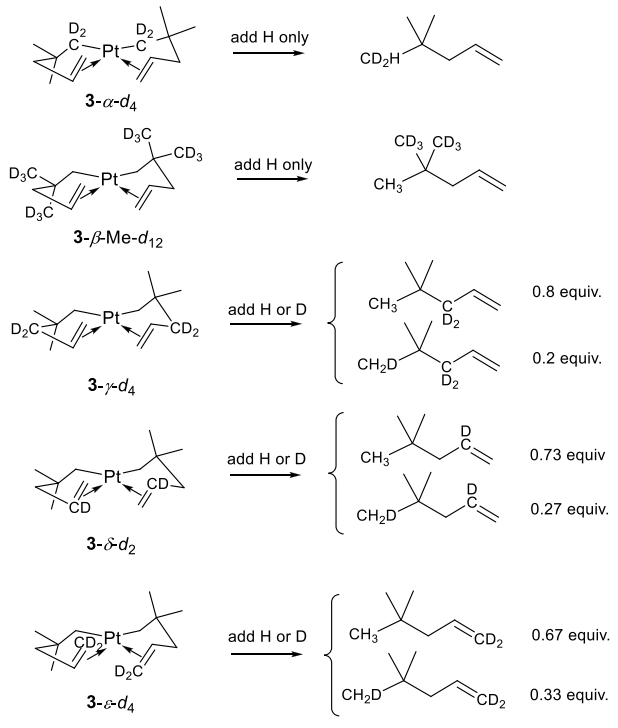

[a]The 1-pentene structure is shown for simplicity, but there is considerable isomerization to the 2-pentene isomer and a small amount of H−D scrambling occurs among the allylic and olefinic (i.e., γ, δ, and ε) positions.

https://dx.doi.org/10.1021/acs.organomet.0c00542
Organometallics 2020, 39, 3817−3829

are formed by adding one D atom to the pentenyl ligands, and the rest are formed by adding one H atom (Table S5.2 and Figures S5.7, S5.18, and S5.24). The results for 3-γ-d_4 and 3-δ-d_2 appear to be different in C_6H_6 than in C_6F_6.

Thus, we reach a somewhat surprising conclusion: there is not one mechanism but at least three principal mechanisms for the thermolysis of **3**—activation of γ-, δ-, and ε-C−H bonds—all operating in parallel at comparable rates. There is a small possibility that not all of these C−H activation processes occur in the primary step: i.e., that activation occurs initially at one or two preferred positions and that activation at the other sites occurs subsequently from the dehydrogenated ligand. The KIE studies below, however, rule out the possibility that activation occurs at only one site.

We note here that the simultaneous activation of γ-, δ-, and ε-C−H bonds over α-C−H bonds has also been seen in the thermolysis of the β-stabilized 2,2-dimethylpentyl compound $Pt(CH_2CMe_2CH_2CH_2CH_3)_2(PEt_3)_2$: 23% of the molecules are thermolyzed by the activation of γ-C−H bonds, 68% by δ-C−H bonds, and 9% by ε-C−H bonds, with relative rates of 2.6:7.6:1.[33] In this system, the thermolysis was proposed to involve dissociation of one of the PEt_3 ligands to generate a three-coordinate (or σ-complex) intermediate, followed by C−H activation to generate a Pt hydride; the hydrogen atom subsequently transfers to the other alkyl ligand.[33]

Assessment of the Extent of Intramolecular H/D Scrambling in Unreacted 3. The multiple C−H bond activation processes that **3** undergoes prompted us to determine whether intramolecular H/D scrambling occurs before the reductive elimination of the 4,4-dimethylpentenes. To do this, we followed the locations of the deuterium labels in unreacted **3** as the thermolysis proceeded. Thermolysis of 3-γ-d_4 in C_6F_6, C_6H_6, and C_6D_6 at 110 °C shows that no deuterium scrambles into the α-position of unreacted **3** (Figures S5.1, S5.3, S5.5, S5.7, and S5.9) and less than 7% of the δ or ε olefinic protons in unreacted **3** become deuterated after 1.5 half-lives. The finding that the extent of H/D scrambling in unreacted **3** is very small affords an important insight into the mechanism of thermolysis, which we will discuss below, but otherwise we can assume that the deuterium labels largely stay in place when **3** is heated.

Isotope Labeling Studies: Kinetic Isotope Effects. The above results show that a key step in the thermolysis of **3** is the activation of C−H bonds. As mentioned above, during thermolysis we see no organoplatinum complexes in solution other than **3**, and the rate constant for generation of the 4,4-dimethylpentenes is the same as the rate constant for the disappearance of **3**. Therefore, the rate-determining step (RDS) must involve **3** or an activated form thereof.

For C−H bond activation processes, there are four possibilities for the RDS (Scheme 6):[49] (1) formation of a CH−M σ complex, (2) oxidative cleavage of a C−H bond, (3) reductive C−H coupling to form the organic byproduct(s), or (4) dissociation of the organic byproducts from the metal center. We already have some evidence that the RDS cannot be step 4, because if it were, there should be significant intramolecular H/D scrambling in unreacted **3** that is specifically deuterium labeled.[50,51] However, very little such scrambling occurs, as mentioned above. Possibility 1 does not involve making or breaking C−H bonds; thus, if the RDS for the thermolysis of **2** is this step, then the rate of thermolysis should not show a primary deuterium kinetic isotope effect (KIE), k_H/k_D. In contrast, if the RDS for the thermolysis of **3** is step 2 or 3, a primary deuterium KIE should be seen. Therefore, valuable mechanistic information can be obtained by measuring the KIE for thermolysis of deuterated isotopologues of **3**.

Scheme 6. Possible Steps in the Decomposition of 3

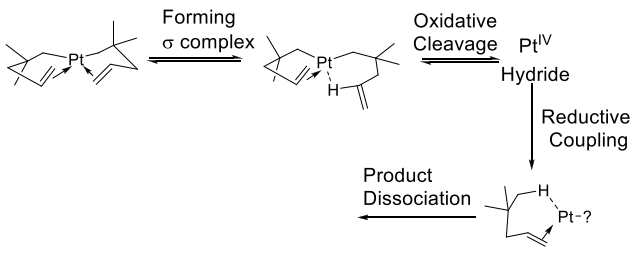

To gain insight into the RDS, we measured the k_H/k_D values for the thermolysis of the three isotopologues of **3** involved in C−H bond cleavage described in the previous section. We determined the k_H/k_D values for 3-γ-d_4, 3-δ-d_2, and 3-ε-d_4 in two ways: from the rate at which **3** disappears over time (as determined from ^{1}H NMR integrals) and from the amount of deuterium present in the *tert*-butyl groups of the product 4,4-dimethylpentenes (as determined from ^{1}H and ^{2}H NMR integrals).

From the rate of disappearance of **3**, the measured k_H/k_D values for 3-γ-d_4, 3-δ-d_2, and 3-ε-d_4 in C_6D_6 are 1.2(1), 1.5(1), and 1.3(1), respectively, and in C_6F_6 are 1.2(1), 1.2(1), and 1.1(1), respectively.[52,53] Thus, the measured k_H/k_D values in C_6D_6 are somewhat larger than those measured in C_6F_6; this result is consistent with the rate and activation parameter data (Figure 1; see above), which suggested that the thermolysis of **3** follows different mechanisms in the two solvents.

The finding that activation of the δ-C−H bonds of **3** in C_6D_6 has a measured k_H/k_D value larger than that for activation of the γ- and ε-C−H bonds can also be seen in NMR spectra taken after a certain fixed thermolysis time. Thus, after 46 h of thermolysis in C_6H_6, 3-δ-d_2 generates significantly less 4,4-dimethylpentene than do 3-γ-d_4 and 3-ε-d_4 (Figure 2).

The relatively small measured k_H/k_D values at first glance seem to be inconsistent with being primary KIEs, and thus we may be tempted to rule out the possibility that steps 2 and 3 are rate-determining. In fact, we need to interpret the small k_H/k_D values in a more global way.

Analysis of the Average KIE for Three Pathways Operating in Parallel, in Which Only One Pathway Involves Deuterated Bonds. The measured k_H/k_D values for the thermolysis of 3-γ-d_4, 3-δ-d_2, and 3-ε-d_4 must be interpreted in light of the facts that (1) the thermolysis of **3** occurs by multiple pathways, all operating in parallel and each involving a different C−H bond, and (2) for the deuterated isotopologues of **3** we investigated, only one of these sites is deuterated. Therefore, at most only one of the three pathways will show a KIE (and then only if this step is rate-determining), whereas the other two pathways have KIE = 1 because those sites are not deuterated; the measured k_H/k_D value will be a weighted average among all three pathways.

For the general case of three C−H activation pathways operating in parallel at different rates, only one of which involves deuterated bonds, let R_1, R_2, and R_3 be the measured (i.e., average) k_H/k_D values for the deuterated isotopologues that are specifically labeled at sites 1−3, respectively. As a starting point, let us assume that the intrinsic KIE for activation

https://dx.doi.org/10.1021/acs.organomet.0c00542
Organometallics 2020, 39, 3817−3829

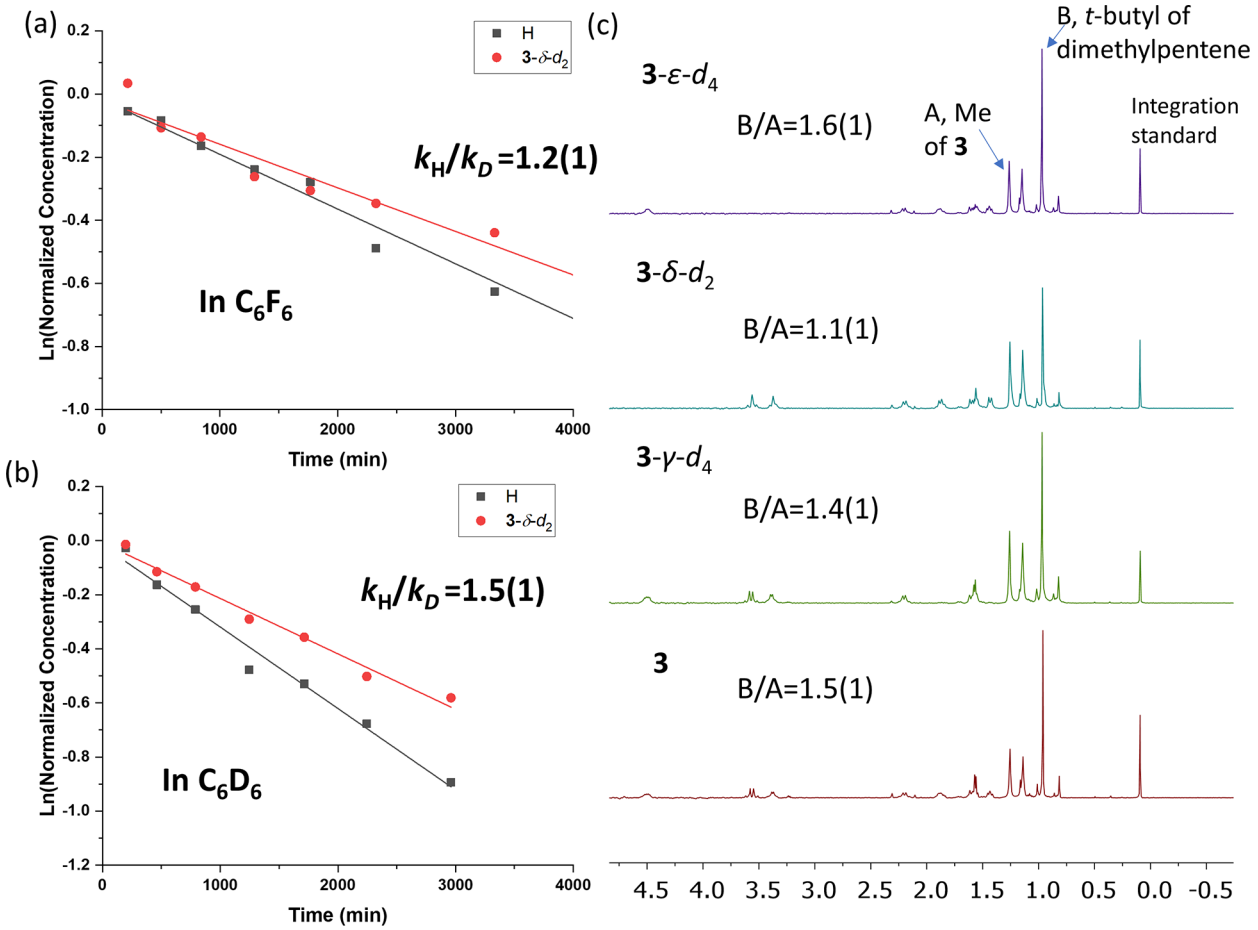

Figure 2. (a) Natural log of normalized concentration (i.e., $C_0 = 1$) vs time for thermolysis of **3** and **3**-δ-d_2 at 110 °C in C_6F_6. (b) Natural log of normalized concentration (i.e., $C_0 = 1$) vs time for thermolysis of **3** and **3**-δ-d_2 at 110 °C in C_6D_6. (c) ^{1}H NMR spectrum of the products of thermolysis of **3**, **3**-γ-d_4, **3**-δ-d_2, and **3**-ε-d_4 at 110 °C in C_6H_6 after 56 h in a side by side experiment, showing the different ratios of the integrals of the methyl resonances of unreacted **3** to that of the product product 4,4-dimethylpentene at this time point.

of a C−H bond vs a C−D bond is the same for all three sites; we will call this value x. We also assume (as is observed) that scrambling of the deuterium labels among the three sites is negligible. Under these assumptions, then $R_1 = (c_1k_{1H} + c_2k_{2H} + c_3k_{3H})/(c_1k_{1H}/x + c_2k_{2H} + c_3k_{3H})$, $R_2 = (c_1k_{1H} + c_2k_{2H} + c_{\varepsilon 3}k_{3H})/(c_1k_{1H} + c_2k_{2H}/x + c_3k_{3H})$, and $R_3 = (c_1k_{1H} + c_2k_{2H} + c_3k_{3H})/(c_1k_{1H} + c_2k_{2H} + c_3k_{3H}/x)$, where the coefficients c_1, c_2, and c_3 reflect the populations of the three sites.

Let us now compute the quantity $1/R_1 + 1/R_2 + 1/R_3$:

$$\frac{1}{R_1} + \frac{1}{R_2} + \frac{1}{R_3} = \frac{c_1k_{1H}/x + c_2k_{2H} + c_3k_{3H}}{c_1k_{1H} + c_2k_{2H} + c_3k_{3H}} + \frac{c_1k_{1H} + c_2k_{2H}/x + c_3k_{3H}}{c_1k_{1H} + c_2k_{2H} + c_3k_{3H}} + \frac{c_1k_{1H} + c_2k_{2H} + c_3k_{3H}/x}{c_1k_{1H} + c_2k_{2H} + c_3k_{3H}}$$

This expression simplifies to $1/R_1 + 1/R_2 + 1/R_3 = 2 + 1/x$, from which we obtain $x = 1/[(1/R_1 + 1/R_2 + 1/R_3) - 2]$. This equation enables us to calculate x, the intrinsic KIE for deuteration of one of the three sites, from the three measured k_H/k_D values (if the assumptions that led to this expression are true).

From this KIE value, we can also calculate the fractional contributions of the three pathways to the overall reaction for the undeuterated compound (assuming that there is no H/D scrambling with other sites after the rate-determining step). We will call these three numbers the branching fractions. Manipulation of the equation $R_1 = (c_1k_{1H} + c_2k_{2H} + c_3k_{3H})/(c_1k_{1H}/x + c_2k_{2H} + c_3k_{3H})$ shows that the fraction f_1 of undeuterated **3** that decomposes by pathway 1, i.e., the ratio $c_1k_{1H}/(c_1k_{1H} + c_2k_{2H} + c_3k_{3H})$, is equal to $(1 - 1/R_1)/(1 - 1/x)$; similar expressions give the branching fractions for the other two pathways.

Furthermore, for each of the single-site deuterated isotopologues of **3**, we can predict the mole fraction χ of the 4,4-dimethylpentenes that is formed by adding a deuterium atom: further manipulation of the equation $R_1 = (c_1k_{1H} + c_2k_{2H} + c_3k_{3H})/(c_1k_{1H}/x + c_2k_{2H} + c_3k_{3H})$ shows that $\chi_1 = (c_1k_{1H}/x)/(c_1k_{1H}/x + c_2k_{2H} + c_3k_{3H})$ is equal to $(R_1 - 1)/(x - 1)$; again, similar expressions give the mole fractions expected from the other two isotopologues of **3**. These predictions assume that no further C−H bond activation or H/D scrambling occurs after the initial C−H bond activation step; furthermore, as mentioned above, the entire model is based on the assumption that the intrinsic KIEs for the three sites are approximately equal.

Application of the Above Kinetic Model to the Data for 3 in C_6D_6 and C_6F_6. For thermolysis of **3** in C_6D_6, inserting the measured values $R_\gamma = 1.2(1)$, $R_\delta = 1.5(1)$, and $R_\varepsilon = 1.3(1)$ into the above model affords the following value for the intrinsic KIE for activating a single C−H vs C−D bond: $x = 3.7(9)$. This value falls in the range expected for a primary deuterium KIE for breaking or making a C−H bond.

https://dx.doi.org/10.1021/acs.organomet.0c00542
Organometallics 2020, 39, 3817−3829

The model also predicts that, for thermolysis of the deuterated isotopologues 3-γ-d_4, 3-δ-d_2, and 3-ε-d_4, on a mole fraction basis 0.08(5), 0.19(7), and 0.11(5) of the 4,4-dimethylpentenes, respectively, should be formed by adding one deuterium atom to a pentenyl ligand. Experimentally, as described above, these mole fractions are 0.5(1), 0.15(4), and 0.28(5) for thermolyses of 3-γ-d_4, 3-δ-d_2, and 3-ε-d_4 in C_6H_6. The value for 3-δ-d_2 is in reasonable agreement with the predictions based on the model, but the values for 3-γ-d_4 and 3-ε-d_4 are not. This disagreement suggests that one of the assumptions behind the model is invalid. In particular, as we will show below, the disagreement can be explained if the intrinsic KIEs are different for each site: the results suggest that the KIEs for activation of the γ- and ε-C−H bonds are smaller than 3.7 (i.e., possibly they are secondary KIEs), whereas the KIE for activation of the δ-C−H bonds is larger than 3.7 (i.e., primary).

Interpretation of the KIE Results in Benzene. The results in the previous section suggest that the KIEs for activation of the γ- and ε-C−H bonds may be smaller than the KIE for activation of the δ-C−H bonds. One way in which this difference may arise is as follows. In the most general mechanism, the first two steps in the activation of a C−H bond at a metal center are the formation of C−H σ complex, followed by oxidative addition of the C−H bond (Scheme 7).[49] The rate constants k_1 and k_{-1} that describe the reversible

Scheme 7. One of the Proposed Pathways for Activation of C−H bonds in 3[a]

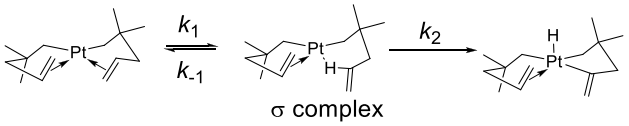

[a]Activation of the δ-C−H bond is shown; the other two pathways involve activation of the γ- and ε-C−H bonds.

formation of the σ complex should have near-unity KIEs because the C−H bond is not broken in these steps and might even be inverse owing to zero-point effects; in contrast, the rate constant k_2 should show a large primary KIE.

As has been pointed out by others,[54] the magnitude of the KIE actually measured in such systems depends on the ratio between k_{-1} and k_2: i.e., on the relative rates with which the σ complex reverts to 3 vs activates a C−H bond. Specifically, if the steady-state assumption is applied to the σ complex, then the first-order rate constant for C−H bond activation is $k_{obs} = k_1k_2/(k_{-1} + k_2)$. If $k_{-1} \gg k_2$, i.e., oxidative addition of the C−H bond (k_2) is slow and therefore the rate-determining step, then $k_{obs} = k_1k_2/k_{-1}$; in this case, a large and primary KIE is expected. If instead $k_2 \gg k_{-1}$, i.e., oxidative addition of the C−H bond (k_2) is fast so that formation of the σ complex is the RDS, then $k_{obs} = k_1$, and a small and possibly inverse KIE is expected.

As a result, large KIEs are expected if cleavage of the C−H bond is the RDS,[33,54,50] whereas small and possibly inverse KIEs are expected if formation of the σ complex is the RDS.[50−56] For 3, the formation of a σ complex with the δ-C−H bond should have a relatively low barrier, because the resulting ring is six-membered and therefore likely to have the lowest strain (taking into account ring strain, transannular strain, and torsional strain). The low barrier for formation of the σ complex means that this step is unlikely to be rate determining, and instead the RDS will be cleavage of the C−H bond; a large and primary KIE is therefore expected, as our kinetic results suggest. In fact, we know from solution studies that 3 undergoes a dynamic "alkene flipping" process that likely proceeds by a nondissociative mechanism (as judged from the activation parameters), probably involving a σ-complex intermediate.[30]

In contrast, the σ complex involving ε-C−H bonds forms seven-membered rings that will be characterized by larger amounts of strain. The σ complex involving the γ-C−H bonds may also be hard to form because these hydrogen atoms are not directly attached to the C═C bond, and the σ complex cannot be directly formed by a nondissociative "alkene flipping" process. As a result, the barrier for formation of the σ complex is more likely to be high and rate-determining. Therefore, for activation of both the γ- and ε-C-H bonds, a small and possibly inverse KIE is expected.

Let us now return to our kinetic model but change the underlying assumption, in an attempt to understand the observed k_H/k_D values: let us assume that activation of C−H bonds at sites 1−3 have different intrinsic KIEs given by x_1, x_2, and x_3. We can then derive the expression $1/R_1 = 1 - f_1(1 - 1/x_1)$, where f_1 is the branching fraction (i.e., the fraction of undeuterated 3 that reacts by pathway 1); analogous expressions apply for pathways 2 and 3. Let us assume that activation of the δ-C−H bonds has an intrinsic KIE of 5 (a reasonable primary value). Then from the 1.5 value of R_δ we can estimate that f_δ is approximately 40%;[57] this estimate does not change much as long as x_1 is much larger than 1. In other words, approximately 40% of undeuterated 3 reacts by activation of δ C−H bonds.

The modified model predicts that, for the isotopologue of 3 deuterated at site 1, the mole fraction of the 4,4-dimethylpentenes that should be formed by adding a deuterium atom to the pentenyl ligands is given by the expression $\chi_1 = 1/(x_1/f_1 + 1 - x_1)$, and similar equations pertain for deuteration at the other two sites. For 3-δ-d_2 in benzene, for which we estimate that the intrinsic KIE $x_\delta = 5$ and the branching fraction $f_\delta = 40\%$, the model predicts that the mole fraction of 4,4-dimethylpentenes that should be generated by addition of a deuterium to the pentenyl ligands is 0.12; the experimental value is 0.15(4). If we assume that the branching fractions for activation of the γ- and ε-C−H bonds of 3 in benzene are 40% and 20%, respectively, and that the intrinsic KIEs for these two pathways are $x_\gamma = x_\varepsilon = 0.7$, then the model predicts that $\chi_\gamma = 0.48$ and $\chi_\varepsilon = 0.26$; the experimental values for the fraction of the 4,4-dimethylpentenes formed by adding a deuterium atom from 3-γ-d_4 and 3-ε-d_4 are 0.5(1) and 0.28(5). These deduced branching fractions and intrinsic KIEs should be considered as illustrative rather than definitive, however, because in benzene the errors in the observed k_H/k_D values are large in comparison to how much the k_H/k_D values differ from 1.

In summary, the measured k_H/k_D and the small amount of deuterium incorporated into the 4,4-dimethylpentene products for the thermolysis of 3-δ-d_2 in benzene suggest that the RDS for activation of the δ-C−H bonds in this solvent involves breaking (or making) a C−H bond and is characterized by a large KIE of about 5.[58] In contrast, the RDS for activation of γ- and ε-C−H bonds is most likely formation of the σ complex that precedes the C−H bond activation step and is

https://dx.doi.org/10.1021/acs.organomet.0c00542
Organometallics 2020, 39, 3817−3829

characterized by a KIE that is close to unity (or possibly inverse).

Interpretation of the KIE Results in Hexafluorobenzene. In contrast to the results above, thermolysis of **3**-γ-d_4, **3**-δ-d_2, and **3**-ε-d_4 in C_6F_6 shows (1) much smaller (and very similar) measured k_H/k_D values of R_γ = 1.2(1), R_δ = 1.2(1), and R_ε = 1.1(1) and (2) very similar deuterium contents in the 4,4-dimethylpentene byproducts. The 4,4-dimethylpentene mole fractions generated by addition of a deuterium to the pentenyl ligands are 0.2(1), 0.27(5), and 0.33(8), respectively. The greater deuterium incorporation seen for thermolysis **3**-δ-d_2 in C_6F_6 (vs that of 0.15 seen in C_6H_6) suggests that the δ-C−H activation pathway has a smaller intrinsic KIE in comparison to thermolysis in C_6H_6. If we assume that all three pathways have the same intrinsic KIE, as the mole fractions above imply, then we calculate that x, the average KIE for activation of a single C−H bond, is 1.7(20). This result suggests that, for all three pathways, the RDS for the thermolysis of **3** in C_6F_6 is probably not cleavage or formation of C−H bonds but something else.

These observations, along with the observation that the first-order rate constant for thermolysis of **3** in C_6F_6 is distinctly slower than in C_6H_6, suggest that C_6F_6 directly affects how **3** undergoes thermolysis.

For C−H activation processes in other systems, it is known that increasing the coordinating ability of the solvent (such as from CH_2Cl_2 to MeCN) can sometimes cause the measured KIE to change from large and primary to small and secondary.[50] The explanation is that in a weakly coordinating solvent the RDS is oxidative cleavage of C−H bond, whereas in a strongly coordinating solvent the solvent competes with (and slows) the coordination of a C−H bond to the metal center. This slowing causes the formation of the C−H σ complex to become rate-determining, and a secondary KIE results.

In both C_6H_6 and C_6F_6, formation of the σ complex appears to be the RDS for γ- and ε-C−H activation. In contrast, for δ-C−H activation, we propose that benzene acts as a weakly coordinating solvent, so that C−H bond cleavage (or formation) is the RDS and a large primary KIE is seen,[59] whereas C_6F_6 is a strongly coordinating solvent, so that formation of the σ complex is the RDS and a small and possibly inverse KIE is seen (Scheme 8).[55,59−51] It is known that C_6F_6 binds more strongly than C_6H_6 to Pt^0 because it is a better π acceptor[64] and that C_6F_6 forms stable η^2 complexes with Ir^I or Rh^I, which are isoelectronic with Pt^{II}.

Scheme 8. Different Mechanisms for Activation of the δ-C−H bonds of 3 in C_6H_6 and C_6F_6

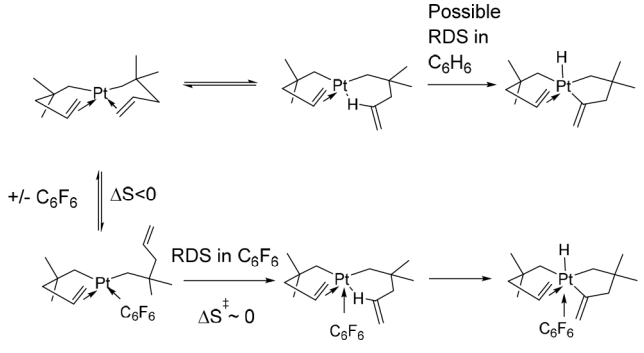

We showed above that, in comparison to the entropy of activation of 11 ± 5 eu for thermolysis of **3** in C_6D_6, the entropy of activation for thermolysis of **3** in C_6F_6 is more negative by 18 ± 6 eu (Figure 2). This value is consistent with association of C_6F_6 before the RDS, because the measured activation parameters in C_6F_6 are not for a single step: it reflects both the thermodynamics of the pre-equilibrium of solvent association before the RDS (which has a negative entropy change) and the thermodynamics of the RDS itself (Scheme 8).

The results support the hypothesis that the association of C_6H_6 plays essentially no role in the thermolysis of **3**, so that the results in this solvent reflect how **3** decomposes unimolecularly. In contrast, C_6F_6 coordinates to Pt and changes both the mechanism and the RDS of the δ-C−H bond activation pathway. Interestingly, the rate of "alkene flipping" is the same in C_7H_8 and C_7F_8 (see section 6 in the Supporting Information), which suggests that coordination of C_6F_6 is not involved in the σ-complex transition state for "alkene flipping" but occurs before the formation of the σ-complex intermediate that leads to C−H activation.

Fate of the Pt Intermediate Formed after C−H Bond Cleavage: Formation of the 4,4-Dimethylpentenes and Platinum-Containing Thermolysis Products. The major decomposition mechanism of **3** involves three pathways, each of which lead to C−H bond cleavage. The cleavage should afford a platinum(IV) species bearing an unmodified pentenyl ligand, a hydride, and a dehydrogenated pentenyl ligand (probably a metallacycle). The subsequent reductive elimination of the pentenyl and hydride ligands forms ∼1 equiv of 4,4-dimethylpentenes and a Pt^{II} complex with a dehydrogenated pentenyl ligand.

A small amount of the dehydrogenated pentenyl ligands rearranges to form the C_7H_{12} species (*E*)-5-methylhexa-1,3-diene, 1,1-dimethyl-3-methylenecyclobutane, and 1,4,4-trimethylcyclobutane, or reacts with benzene to form pentenylbenzene species (Schemes S3.1 and S3.2). The release of these organic byproducts, however, is inefficient under solution thermolysis conditions,[33,65] and most of the dehydrogenated pentenyl ligands are retained in the black Pt-containing solids that are also formed.

Comparison between Thermolysis of 1 and 3 in Solution. Some years ago we described the highly volatile platinum(II) pentenyl compound $Pt[(CH_2)_3CH{=}CH_2]_2$ (**1**), an analogue of **3**, and showed that it could be used to deposit platinum thin films by chemical vapor deposition (CVD).[66] This precursor is air- and water-stable and also has an unusually high vapor pressure for an organoplatinum compound but decomposes over time at room temperature. We showed that one of the key steps in the decomposition mechanism is β-hydrogen elimination, a process that for transition metals often has a low barrier.[67−70]

It is well-known that blocking β-hydrogen elimination leads to a significant improvement in the thermal stability of transition-metal alkyls.[67−70] At 87 °C in toluene-d_8, the rate constant for thermolysis of the non-methylated analogue **1** is 2.5×10^{-2} min^{-1}.[66] For comparison, the rate constant for thermolysis of **3** at 89.5 °C in benzene-d_6 is $2.1(2) \times 10^{-5}$ min^{-1}; thus, replacing the two β-hydrogen atoms with two β-methyl groups leads to a decrease in the rate of thermolysis by ∼3 orders of magnitude.

In addition to the improving the thermal stability by changing the thermolysis mechanism, substitution of β-H

https://dx.doi.org/10.1021/acs.organomet.0c00542
Organometallics 2020, 39, 3817−3829

atoms with methyl groups also changes the nature of the thermolysis products. Thermolysis of **1** in benzene generates ~1.3 equiv of pentene isomers (hydrogenated ligands) and ~0.4 equiv of pentadiene isomers (dehydrogenated ligands). In total, 1.7 equiv of pentenyl-derived organic byproducts is generated per equivalent of **1**. In contrast, thermolysis of **3** generates ~1 equiv of hydrogenated pentenyl ligands and ~0.1 equiv of dehydrogenated ligands. (Table S8.3).

Comparison of Byproducts Formed by Thermolysis of 3 in Solution and under Static CVD Conditions. We previously showed that, under static[41] hot-wall CVD conditions,[30] the thermolysis of **3** at 250 °C gives the products shown in Scheme 9, given in moles per mole of **3**, as determined by GC-MS and ^{1}H NMR analyses. This product distribution accounts for essentially 100% of the carbon and hydrogen atoms in **3**, all of which are converted into volatile byproducts except for a small amount of carbon, which remains on the surface:

Scheme 9. Thermolysis Products Generated from 3 under Static CVD Conditions[a]

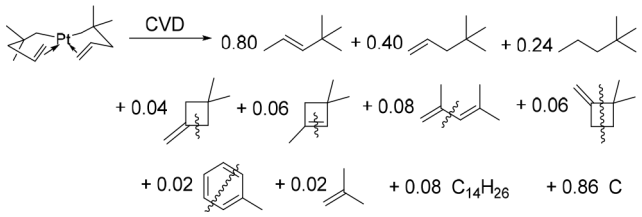

[a]Products that are the result of skeletal rearrangements are indicated with wavy lines at the places where C−C bond cleavage and formation occur.

Relative to the organic products seen under CVD conditions at 250 °C, thermolysis of **3** in benzene near 120 °C shows no formation of the multiply hydrogenated product 2,2-dimethylpentane. In addition, fewer organic species are generated by dehydrogenation of the pentenyl ligands in **3**, and the amounts of these dehydrogenated species are smaller. These findings show that, not unexpectedly, more of the carbon atoms (and some of the hydrogen atoms) are retained in the black precipitate formed when **3** is thermolyzed at ~120 °C in solution than are retained in the films deposited at 250 °C under CVD conditions.

For those dehydrogenated pentenyl ligands that are released from Pt, the majority are formed by skeletal rearrangements that involve C−C bond cleavage; this is because the dehydrogenated ligands have no easy pathway to desorb from the surface by C−H bond activation because the 2,2-dimethyl substituents block low-energy processes such as β-hydrogen elimination and formation of conjugated dienes. Thus, the only way in which the dehydrogenated ligands from **3** can desorb from the surface is by breaking or forming C−C bonds. Although such processes are known to occur on Pt surfaces,[71] they are slow, and as a result the surface becomes poisoned by the dehydrogenated pentenyl ligands.[30]

Energy Barrier of CVD vs Energy Barrier in Solution. In the absence of reactive gases, deposition from **3** generates smooth nanocrystalline Pt films that contain 40−50% carbon.[30] The growing Pt surface is most likely covered with hydrocarbons;[72,73] for growth from **3** the dehydrogenated ligands serve as poisons that considerably reduce the catalytic activity of the Pt surface. On such a surface, the thermolysis of **3** probably involves adsorption from the gas phase followed by a unimolecular process (Scheme 10).

Scheme 10. Possible Decomposition Mechanism of 3 on a Poisoned Pt Surface during CVD

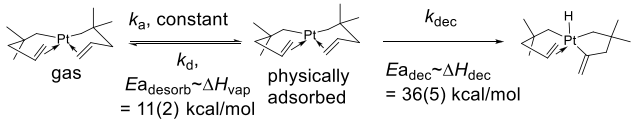

The rate of decomposition of **3** on the poisoned Pt surface can be written as $k = k_a k_{dec}/k_d$, in which k_a and k_d are the rates of adsorption and desorption, respectively, and k_{dec} is the rate of unimolecular decomposition. Because the adsorption step is barrierless, the activation energy for deposition of films of **3**, E_a(depos), can be derived from the activation energy for desorption of **3**, E_a(desorb), and the activation energy of unimolecular decomposition of **3**, E_a(dec):

$$E_a(\text{depos}) = -E_a(\text{desorb}) + E_a(\text{dec})$$

Because the growing Pt surface during CVD is covered with hydrocarbons, and **3** is a hydrocarbon-like molecule, we assume that E_a(desorb) is similar to the heat of vaporization of **3**,[74] which we previously measured to be 11(2) kcal/mol.[30] Let us assume that E_a(dec) is similar to $\Delta H^{\ddagger}$ for thermolysis of **3** in C_6D_6, which we showed above is 36 (5) kcal/mol (we assume here that the behavior of **3** in a hydrocarbon solvent resembles its behavior on a hydrocarbon-rich surface). From these crude assumptions, we estimate that E_a(depos) for deposition from **3** should be approximately 25 (5) kcal/mol on a chemically inert surface. This value is comparable to the activation energy of 18 (3) kcal/mol for thermolysis of **3** under CVD conditions.[30] This barrier for the unimolecular decomposition of **3** on surfaces is relatively small and is responsible for the fast nucleation seen for **3** when it is used as a CVD precursor.

Note that, in contrast, the commercial precursor $(C_5H_4Me)PtMe_3$ has no low-barrier pathways for decomposition. Computational studies suggest that the $Pt^{IV}-CH_3$ bond is strong (51 kcal/mol),[75] which is significantly larger than the measured enthalpy of activation for **3**; the $Pt-C_5H_4Me$ bond is certainly even stronger. Thus, the nucleation of $(C_5H_4Me)PtMe_3$ probably is not initiated by dissociation of a ligand but instead by reaction with surface hydroxy groups.[22] As a result, the nucleation behavior of $(C_5H_4Me)PtMe_3$ shows a strong dependence on the nature of the underlying substrate.[76] The nucleation behavior of **3**, in contrast, does not appear to show substrate dependence, although this observation does not necessarily rule out the possibility that **3** also nucleates by reaction with surface hydroxyl groups.[30]

CONCLUDING REMARKS

Thermolyses of **3** in solution and under CVD conditions both produce large amounts of 4,4-dimethyl-1-pentene, much of which is isomerized to its isomer 4,4-dimethyl-2-pentene; both products are the result of adding a hydrogen atom to the dimethylpentenyl ligands in **3**. The additional hydrogen atom arises by C−H activation of other dimethylpentenyl ligands. For thermolysis in solution, we have shown that the extra hydrogen comes from the olefinic and allylic hydrogen atoms of the other ligand of the same molecule. For thermolysis

https://dx.doi.org/10.1021/acs.organomet.0c00542
Organometallics 2020, 39, 3817−3829

under static CVD conditions, the extra hydrogen comes from the dehydrogenation of pentenyl ligands on the platinum surface.

In hydrocarbon solvents such as C_6D_6, the mechanism of C−H bond activation involves three pathways, operating in a simultaneous manner and in parallel. The first step is decomplexation of the C═C bond of one of the ligands of **3** to generate a σ complex in which an allylic γ-C−H bond or an olefinic δ- or ε-C−H bond coordinates to Pt. Subsequently, C−H activation of one of these C−H bonds occurs to form a short-lived Pt^{IV} hydride, which reductively eliminates ∼1 equiv of 4,4-dimethylpentenes and generates an insoluble black precipitate that contains most of the dehydrogenated pentenyl ligands.

For activation of the γ- and ε-C−H bonds, the RDS is formation of the σ complex. In contrast, for activation of the δ-C−H bonds the RDS is intramolecular C−H bond oxidative cleavage (or formation) in C_6H_6 but formation of the σ complex in C_6F_6, as shown by a series of studies involving deuterated isotopologues of **3**. We attribute the change of mechanism to the stronger coordinating ability of C_6F_6, which coordinates to Pt and hinders the formation of the C−H σ complex, whereas C_6H_6 does not participate significantly in the decomposition before or during the RDS (but does become slightly involved afterward). Thus, the thermolysis pathway in benzene reasonably models the mechanism by which **3** decomposes under CVD conditions on an inert surface (i.e., unimolecularly).

Although there are dangers associated with extrapolating results in solution to processes (such as CVD) that occur in the absence of solvent, under the right circumstances the chemistry of organometallic molecules in solution can afford an important insight into the chemistry behind CVD processes.[77] Here, the hydrocarbon solvents we have used play essentially no role in the chemistry, and it seems reasonable to use the thermolysis studies as a basis for formulating hypotheses about why some precursors give smooth Pt films and others do not. For precursors such as $(C_5H_4Me)PtMe_3$, which have no low-energy pathway to dissociate a ligand, the formation of nuclei is slow but the growth on Pt (which can catalyze the loss of ligands) is fast; these circumstances lead to a low density of nuclei and the formation of rough films. For compound **3**, however, a C═C bond can readily decomplex to form intermediates that can readily convert to growth species, so that the formation of nuclei is fast on all surfaces; in addition, the dehydrogenated pentenyl ligands poison the Pt surface.[30] As a result, the Pt-containing films grown from **3** are unusually smooth.

Detailed studies of the use of **3** as a CVD precursor are described in a separate paper.[30]

EXPERIMENTAL SECTION

All manipulations were carried out under vacuum or under argon using standard Schlenk techniques unless otherwise specified. All glassware was oven-dried before use. Hexamethyldisiloxane (Petrarch Systems) and perfluorotoluene (Sigma-Aldrich) were used as received, 1,2,4,5-tetrachlorobenzene (Eastman Chemical) was recrystallized from diethyl ether, and hexafluorobenzene (Strem Chemicals) was dried over 3 Å molecular sieves. Benzene-d_6 (Cambridge Isotope Laboratories) and benzene (EMD Millipore) were distilled under nitrogen from sodium/benzophenone, and cyclohexane-d_{12} was purchased from Cambridge Isotope Laboratories in 1 mL ampules and used without purification.

All isotopologues of **3** were synthesized from the corresponding deuterium-labeled 5-bromo-4,4-dimethyl-1-pentenes. Because these syntheses were conducted on small scales, two modifications of the standard preparations were made in order to obtain reasonable yields. First, the deuterated alcohols were not prepared by direct bromination from deuterated 2,2-dimethylpent-4-en-1-ol, but instead were first converted to the corresponding tosylates and then converted to the bromide with NaBr/HMPA. Second, in order to minimize adventitious oxidation or hydrolysis, lithium reagents were used instead of Grignard reagents to synthesize **3**.[78] The syntheses of the isotopically labeled compounds are described in detail in the Supporting Information.

Thermolysis reactions were conducted in a Thermo Scientific Lindberg/Blue M Mini-Mite Tube Furnace or (for kinetic experiments requiring better temperature control) in a Fisher Scientific Isotemp 1006S refrigerated circulating bath with mineral oil as a heat transfer medium. The 1D ^1H, ^2H, and ^{13}C NMR data were recorded on a Varian Inova 400 spectrometer at 9.39 T, a Varian Inova 500 spectrometer at 11.74 T, a Varian Inova 600 spectrometer at 14.09 T, or a Bruker B500 NMR spectrometer at 11.74 T. Chemical shifts are reported in δ units (positive shifts to higher frequency) relative to TMS (^1H, ^{13}C), set by assigning appropriate shifts to residual solvent signals. GC-MS spectra were collected by the staff of the Roy J. Carver Biotechnology Center at the University of Illinois on a GC/MS system (Agilent Inc., Palo Alto, CA, USA) consisting of an Agilent 7890 gas chromatograph, an Agilent 5975 mass-selective detector, and a HP 7683B autosampler. Peaks were evaluated using the AMDIS 2.71program (NIST, Gaithersburg, MD, USA) and identified with the aid of the libraries NIST08 (NIST, MD, USA) and W8N08 (Palisade Corporation, NY, USA).

Thermolysis of 3 in C_6F_6, C_6D_{12}, C_6D_6, and C_6H_6 Solutions. In order to suppress secondary reactions with colloidal platinum species,[43] we added a drop of mercury to all solutions in which thermolysis studies were conducted. We confirmed by GC-MS that dialkylmercury compounds were not formed (Figure S3.4). The addition of Hg inhibits H−D exchange between byproducts and solvents. A solution of hexamethyldisiloxane or 1,2,4,5-tetrachlorobenzene dissolved in C_6D_6 and sealed in a glass capillary was used as an integration standard. The capillary and the mercury droplet were loaded into an NMR tube, which was evacuated for 5 h at 10 mTorr before addition of analyte.

A sample of **3** (typically 20 mg, 0.051 mmol) was cooled to 0 °C and evacuated for 5 h (10 mTorr) to ensure that it was free of residual solvents. The dried sample was dissolved in the desired solvent (C_6D_6 or C_6F_6; 650 μL), and the resulting solution was transferred to the NMR tube containing the capillary and a drop of mercury. The NMR tube was then degassed by the freeze−pump−thaw technique and flame-sealed under vacuum. The tube was completely immersed in a circulating oil bath preheated to the desired temperature, which could be controlled to within ±1 °C. Multiple measurements at 110 ± 1 °C in the circulating oil bath show that the measured rate constant has a standard deviation of ∼10%. A few nonquantitative thermolysis experiments were conducted by placing the NMR entirely within the hot zone of a tube furnace whose two ends were blocked with glass wool.

At certain time intervals, the NMR tube was removed, cooled to 20 °C to quench the reaction, and examined by NMR spectroscopy. The progress of the reaction was monitored by measuring the peak integrals; the disappearance of **3** due to thermolysis was best followed by integration of the olefinic peaks. The concentration of **3** at $t = 0$ is often somewhat anomalous, possibly due to slow redissolution of the integration standard after the freeze−pump−thaw step. As a result, this data point was omitted from the curve-fitting analyses. Thermolyses were conducted for no more than 2 half-lives to minimize any inhibition effect from byproducts.

To minimize experimental error, experiments were conducted as much as possible in a side by side fashion, with the parameter of interest as the only variable. For example, for deuterium labeling and kinetic isotope studies, deuterated and undeuterated samples of **3** (typically 20 mg, 0.05 mmol) were dissolved separately in the desired

https://dx.doi.org/10.1021/acs.organomet.0c00542
Organometallics 2020, 39, 3817−3829

solvent (C_6D_6 or C_6F_6; 650 μL), and the solutions were transferred to separate NMR tubes, each containing a drop of mercury and a capillary containing an integration standard, as described above. The NMR tubes were flame-sealed and then placed side by side in the same heating bath or hot zone.

For **3**-α-d_4, **3**-γ-d_4, **3**-δ-d_2, and **3**-ε-d_4, the amount of deuterium incorporated into the *tert*-butyl group of the 4,4-dimethylpentene thermolysis products was calculated from ^{2}H NMR peak integrals of unreacted **3** (giving moles of unreacted **3**, parameter A), ^{2}H NMR peak integrals in the *tert*-butyl group (giving moles of $C_3H_5CMe_2CH_2D$, parameter B), and the mole fraction of **3** initially present that had undergone thermolysis (parameter C). The amount of deuterium incorporated into the *tert*-butyl group of the 4,4-dimethylpentene thermolysis products is then given by the expression $B(1 - C)/AC$ (see section 5 in the Supporting Information). For **1**-β-Me-d_{12}, the amount of additional deuterium incorporated into the *tert*-butyl group of the 4,4-dimethylpentene thermolysis products was determined from ^{1}H NMR peak integrals (see section 5 in the Supporting Information). Because the sample of **3**-γ-d_4 contained about 10% of the **3**-α-d_4 isomer (and vice versa for the sample of **3**-α-d_4) owing to scrambling during the preparation of the organolithium reagent,[78] the amount of deuterium in the *tert*-butyl group of the 4,4-dimethylpentene thermolysis products was corrected accordingly, but as a result the KIEs and deuterium contents are less accurate for thermolyses of these two compounds. To ensure the accuracy of NMR integrations, T_1 relaxation times were measured, and recycle delay times larger than $5T_1$ were used.

■ ASSOCIATED CONTENT

Supporting Information

The Supporting Information is available free of charge at https://pubs.acs.org/doi/10.1021/acs.organomet.0c00542.

> Syntheses and characterization of deuterium labeled isotopologues of *cis*-bis(η^1,η^2-2,2-dimethylpent-4-en-1-yl)platinum, supporting data (^{1}H, ^{2}H, ^{13}C, ^{19}F, COSY, and HSQC NMR and GC-MS spectra, kinetic traces, Eyring plots) for the analysis of reaction order, reaction stoichiometry, and other mechanistic details of thermolysis of *cis*-bis(η^1,η^2-2,2-dimethylpent-4-en-1-yl)platinum (**3**) in solution, assignments of decomposition products, and brief discussions of the mechanism of byproduct formation, supporting data (^{1}H NMR spectra and kinetic traces) for the inhibition of the thermolysis rate by added 4,4-dimethylpentene, quantitative ^{1}H and ^{2}H NMR spectra and kinetic traces for deuterium labeling studies, with descriptions of the calculation and of KIE and the amount of extra deuterium incorporated into the *tert*-butyl group of 4,4-dimethylpentene isomers, ^{1}H VT-NMR spectra, NMR line shape fitting, and Eyring plot for "alkene flipping" of **3** in perfluorotoluene, ^{1}H, ^{2}H, and ^{13}C NMR spectra of deuterium-labeled isotopologues of **3**, comparison of the thermolysis of **3** in solution and the gas phase with the behavior of its nonmethylated analogue **1** (PDF)

■ AUTHOR INFORMATION

Corresponding Author

Gregory S. Girolami − *School of Chemical Sciences, University of Illinois at Urbana−Champaign, Urbana, Illinois 61801, United States;* orcid.org/0000-0002-7295-1775; Email: girolami@scs.illinois.edu

Authors

Sumeng Liu − *School of Chemical Sciences, University of Illinois at Urbana−Champaign, Urbana, Illinois 61801, United States;* orcid.org/0000-0002-2133-2122

Zhejun Zhang − *Department of Materials Science and Engineering, University of Illinois at Urbana−Champaign, Urbana, Illinois 61801, United States*

John R. Abelson − *Department of Materials Science and Engineering, University of Illinois at Urbana−Champaign, Urbana, Illinois 61801, United States*

Complete contact information is available at: https://pubs.acs.org/10.1021/acs.organomet.0c00542

Author Contributions

All authors have given approval to the final version of the manuscript.

Notes

The authors declare the following competing financial interest(s): One patent related to this work has been filed: "Metal Complexes for Depositing Films and Method of Making and Using the Same", U.S. Patent Application 20190077819 (Published March 14th, 2019).

■ ACKNOWLEDGMENTS

We thank the National Science Foundation under grants CHE 1665191 and CHE 1954745 (to G.S.G.) and CMMI 1825938 (to J.R.A.) for support of this research.

■ REFERENCES

(1) Pierson, H. O. Introduction and General Considerations. In *Handbook of Chemical Vapor Deposition*; Pierson, H. O., Ed.; William Andrew Publishing: Oxford, 1992; pp 1−16.

(2) Green, M. L.; Levy, R. A. Chemical Vapor Deposition of Metals for Integrated Circuit Applications. *JOM* **1985**, *37*, 63−71.

(3) Hampden-Smith, M. J.; Kodas, T. T. Chemical Vapor Deposition of Metals: Part 1. An Overview of CVD Processes. *Chem. Vap. Deposition* **1995**, *1*, 8−23.

(4) Doppelt, P. Why is Coordination Chemistry Stretching the Limits of Micro-Electronics Technology? *Coord. Chem. Rev.* **1998**, *178−180*, 1785−1809.

(5) Jones, A. C.; Hitchman, M. L., Overview of Chemical Vapour Deposition. In *Chemical Vapour Deposition: Precursors, Processes and Applications*; Jones, A. C., Hitchman, M. L., Eds.; The Royal Society of Chemistry: Cambridge, 2009; pp 1−36.

(6) Hämäläinen, J.; Ritala, M.; Leskelä, M. Atomic Layer Deposition of Noble Metals and Their Oxides. *Chem. Mater.* **2014**, *26*, 786−801.

(7) George, S. M. Atomic Layer Deposition: An Overview. *Chem. Rev.* **2010**, *110*, 111−131.

(8) Bernal Ramos, K.; Saly, M. J.; Chabal, Y. J. Precursor Design and Reaction Mechanisms for the Atomic Layer Deposition of Metal Films. *Coord. Chem. Rev.* **2013**, *257*, 3271−3281.

(9) Aaltonen, T.; Ritala, M.; Sajavaara, T.; Keinonen, J.; Leskelä, M. Atomic Layer Deposition of Platinum Thin Films. *Chem. Mater.* **2003**, *15*, 1924−1928.

(10) Fang, Q.; Hodson, C.; Xu, C.; Gunn, R. Nucleation and Growth of Platinum Films on High-k/Metal Gate Materials by Remote Plasma and Thermal ALD. *Phys. Procedia* **2012**, *32*, 551−560.

(11) Hiratani, M.; Nabatame, T.; Matsui, Y.; Imagawa, K.; Kimura, S. Platinum Film Growth by Chemical Vapor Deposition Based on Autocatalytic Oxidative Decomposition. *J. Electrochem. Soc.* **2001**, *148*, C524−C527.

(12) Baum, T. H.; Comita, P. B. Laser-Induced Chemical Vapor Deposition of Metals for Microelectronics Technology. *Thin Solid Films* **1992**, *218*, 80−94.

(13) Hierso, J.-C.; Serp, P.; Feurer, R.; Kalck, P. MOCVD of Rhodium, Palladium and Platinum Complexes on Fluidized Divided Substrates: Novel Process for One-Step Preparation of Noble-Metal Catalysts. *Appl. Organomet. Chem.* **1998**, *12*, 161−172.
(14) Dossi, C.; Psaro, R.; Bartsch, A.; Fusi, A.; Sordelli, L.; Ugo, R.; Bellatreccia, M.; Zanoni, R.; Vlaic, G. Chemical Vapor Deposition of Platinum Hexafluoroacetylacetonate Inside KL Zeolite: A New Route to Nonacidic Platinum-in-Zeolite Catalysts. *J. Catal.* **1994**, *145*, 377−383.
(15) Serp, P.; Kalck, P.; Feurer, R. Chemical Vapor Deposition Methods for the Controlled Preparation of Supported Catalytic Materials. *Chem. Rev.* **2002**, *102*, 3085−3128.
(16) Choi, D. S.; Robertson, A. W.; Warner, J. H.; Kim, S. O.; Kim, H. Low-Temperature Chemical Vapor Deposition Synthesis of Pt−Co Alloyed Nanoparticles with Enhanced Oxygen Reduction Reaction Catalysis. *Adv. Mater.* **2016**, *28*, 7115−7122.
(17) Ryan, M. Platinum in Next-Generation Materials for Data Storage. *Platinum Met. Rev.* **2010**, *54*, 244−249.
(18) Dorovskikh, S. I.; Zharkova, G. I.; Turgambaeva, A. E.; Krisyuk, V. V.; Morozova, N. B. Chemical Vapour Deposition of Platinum Films on Electrodes for Pacemakers: Novel Precursors and Their Thermal Properties. *Appl. Organomet. Chem.* **2017**, *31*, e3654.
(19) Woodward, B. K., Platinum Group Metals (PGMs) for Permanent Implantable Electronic Devices. In *Precious Metals for Biomedical Applications*; Baltzer, N., Copponnex, T., Eds.; Woodhead Publishing: Sawston, Cambridge, 2014; pp 130−147.
(20) Morcos, B. M.; O'Callaghan, J. M.; Amira, M. F.; Van Hoof, C.; Op de Beeck, M. Electrodeposition of Platinum Thin Films as Interconnects Material for Implantable Medical Applications. *J. Electrochem. Soc.* **2013**, *160*, D300−D306.
(21) Baker, L.; Cavanagh, A. S.; Seghete, D.; George, S. M.; Mackus, A. J. M.; Kessels, W. M. M.; Liu, Z. Y.; Wagner, F. T. Nucleation and Growth of Pt Atomic Layer Deposition on Al_2O_3 Substrates Using (Methylcyclopentadienyl)-trimethyl Platinum and O_2 Plasma. *J. Appl. Phys.* **2011**, *109*, No. 084333.
(22) Xue, Z.; Thridandam, H.; Kaesz, H. D.; Hicks, R. F. Organometallic Chemical Vapor Deposition of Platinum. Reaction Kinetics and Vapor Pressures of Precursors. *Chem. Mater.* **1992**, *4*, 162−166.
(23) Dendooven, J.; Ramachandran, R. K.; Devloo-Casier, K.; Rampelberg, G.; Filez, M.; Poelman, H.; Marin, G. B.; Fonda, E.; Detavernier, C. Low-Temperature Atomic Layer Deposition of Platinum Using (Methylcyclopentadienyl)trimethylplatinum and Ozone. *J. Phys. Chem. C* **2013**, *117*, 20557−20561.
(24) Mackus, A. J. M.; Verheijen, M. A.; Leick, N.; Bol, A. A.; Kessels, W. M. M. Influence of Oxygen Exposure on the Nucleation of Platinum Atomic Layer Deposition: Consequences for Film Growth, Nanopatterning, and Nanoparticle Synthesis. *Chem. Mater.* **2013**, *25*, 1905−1911.
(25) Mackus, A. J. M.; Leick, N.; Baker, L.; Kessels, W. M. M. Catalytic Combustion and Dehydrogenation Reactions during Atomic Layer Deposition of Platinum. *Chem. Mater.* **2012**, *24*, 1752−1761.
(26) Baker, L.; Cavanagh, A. S.; Yin, J.; George, S. M.; Kongkanand, A.; Wagner, F. T. Growth of Continuous and Ultrathin Platinum Films on Tungsten Adhesion Layers Using Atomic Layer Deposition Techniques. *Appl. Phys. Lett.* **2012**, *101*, 111601.
(27) Lien, C.; Konh, M.; Chen, B.; Teplyakov, A. V.; Zaera, F. Gas-Phase Electron-Impact Activation of Atomic Layer Deposition (ALD) Precursors: $MeCpPtMe_3$. *J. Phys. Chem. Lett.* **2018**, *9*, 4602−4606.
(28) Erkens, I. J. M.; Verheijen, M. A.; Knoops, H. C. M.; Keuning, W.; Roozeboom, F.; Kessels, W. M. M. Plasma-Assisted Atomic Layer Deposition of Conformal Pt Films in High Aspect Ratio Trenches. *J. Chem. Phys.* **2017**, *146*, No. 052818.
(29) Lee, W.-J.; Wan, Z.; Kim, C.-M.; Oh, I.-K.; Harada, R.; Suzuki, K.; Choi, E.-A.; Kwon, S.-H. Atomic Layer Deposition of Pt Thin Films Using Dimethyl (*N*,*N*-Dimethyl-3-Butene-1-Amine-*N*) Platinum and O_2 Reactant. *Chem. Mater.* **2019**, *31*, 5056−5064.
(30) Liu, S.; Zhang, Z.; Gray, D.; Zhu, L.; Abelson, J. R.; Girolami, G. S. "Platinum ω-Alkenyl Compounds as Chemical Vapor Deposition Precursors. Synthesis and Characterization of Pt-$[CH_2CMe_2CH_2CH{=}CH_2]_2$ and the Impact of Ligand Design on the Deposition Process", *Chem. Mater.*, in press. DOI: 10.1021/acs.chemmater.0c03226
(31) Foley, P.; DiCosimo, R.; Whitesides, G. M. Mechanism of Thermal Decomposition of Dineopentylbis(triethylphosphine)-platinum(II): Formation of Bis(triethylphosphine)-3,3-dimethylplatinacyclobutane. *J. Am. Chem. Soc.* **1980**, *102*, 6713−6725.
(32) Brainard, R. L.; Miller, T. M.; Whitesides, G. M. Mechanisms of Thermal Decomposition of *trans*-Chloroneopentylbis-(tricyclopentylphosphine)platinum(II). *Organometallics* **1986**, *5*, 1481−1490.
(33) DiCosimo, R.; Moore, S. S.; Sowinski, A. F.; Whitesides, G. M. Cyclometalation of Dialkylbis(triethylphosphine)platinum(II) Complexes: Formation of *Pt*,*Pt*-Bis(triethylphosphine)platinacycloalkanes. *J. Am. Chem. Soc.* **1982**, *104*, 124−133.
(34) Flood, T. C.; Bitler, S. P. Reversible Formal Alkene Insertion into a Chelated Platinum-Alkyl Bond. *J. Am. Chem. Soc.* **1984**, *106*, 6076−6077.
(35) Ermer, S. P.; Struck, G. E.; Bitler, S. P.; Richards, R.; Bau, R.; Flood, T. C. Kinetics and Conformation in the Reversible Insertion of an Alkene into a Platinum-Carbon Bond in a Chelated (Pentenyl)-platinum Complex. *Organometallics* **1993**, *12*, 2634−2643.
(36) Zhugralin, A. R.; Kobylianskii, I. J.; Chen, P. Experimental Gas-Phase and in Silico Investigation of β-Methyl Elimination from Cationic Palladium Alkyl Species. *Organometallics* **2015**, *34*, 1301−1306.
(37) O'Reilly, M. E.; Dutta, S.; Veige, A. S. β-Alkyl Elimination: Fundamental Principles and Some Applications. *Chem. Rev.* **2016**, *116*, 8105−8145.
(38) Brandow, C. G.; Mendiratta, A.; Bercaw, J. E. Ancillary Ligand and Olefin Substituent Effects on Olefin Dissociation for Cationic Zirconocene Complexes Bearing a Coordinated Pendant Olefin. *Organometallics* **2001**, *20*, 4253−4261.
(39) Thomson, S. K.; Young, G. B. Thermolytic Rearrangement of *cis*-Bis(phosphine)bis((trimethylsilyl)methyl)platinum(II) Complexes via β-Alkyl Transfer. *Organometallics* **1989**, *8*, 2068−2070.
(40) Shekhar, S.; Hartwig, J. F. Distinct Electronic Effects on Reductive Eliminations of Symmetrical and Unsymmetrical Bis-Aryl Platinum Complexes. *J. Am. Chem. Soc.* **2004**, *126*, 13016−13027.
(41) Cheon, J.; Dubois, L. H.; Girolami, G. S. Mechanistic Studies of the Thermolysis of Tetraneopentyltitanium(IV). 2. Solid State and Ultra-High-Vacuum Studies of the Chemical Vapor Deposition of TiC Films. *J. Am. Chem. Soc.* **1997**, *119*, 6814−6820.
(42) Jeffries, P. M.; Dubois, L. H.; Girolami, G. S. Metal-Organic Chemical Vapor Deposition of Copper and Copper(I) Oxide from Copper(I) *tert*-Butoxide. *Chem. Mater.* **1992**, *4*, 1169−1175.
(43) Whitesides, G. M.; Hackett, M.; Brainard, R. L.; Lavalleye, J. P. P. M.; Sowinski, A. F.; Izumi, A. N.; Moore, S. S.; Brown, D. W.; Staudt, E. M. Suppression of Unwanted Heterogeneous Platinum(0)-Catalyzed Reactions by Poisoning with Mercury(0) in Systems Involving Competing Homogeneous Reactions of Soluble Organoplatinum Compounds: Thermal Decomposition of Bis-(triethylphosphine)-3,3,4,4-tetramethylplatinacyclopentane. *Organometallics* **1985**, *4*, 1819−1830.
(44) Biswas, S. Mechanistic Understanding of Transition-Metal-Catalyzed Olefin Isomerization: Metal-Hydride Insertion-Elimination vs. π-Allyl Pathways. *Comments Inorg. Chem.* **2015**, *35*, 300−330.
(45) These are the amounts formed at an initial concentration of **3** of 0.08 M. At an initial concentration of 0.24 M, 1,1-dimethyl-3-methylenecyclobutane is consumed during the latter stages of the thermolysis, coincident with the generation of C_6F_5H, possibly by reacting with colloidal Pt.
(46) Russell, S. K.; Lobkovsky, E.; Chirik, P. J. Iron-Catalyzed Intermolecular $[2\pi + 2\pi]$ Cycloaddition. *J. Am. Chem. Soc.* **2011**, *133*, 8858−8861.
(47) For thermolysis in C_6F_6, this behavior can be attributed to inhibition by the olefinic byproducts: when **3** is thermolyzed in C_6F_6 at 110 °C in the presence of 0.21 M (~4 equiv) of 4,4-dimethyl-1-

pentene, the initial rate of thermolysis is reduced by ~20%. (Figure S4.1) In contrast, when **3** is thermolyzed in C_6D_6 in the presence of 0.21 M (~4 equiv) of 4,4-dimethyl-1-pentene, the initial rate of thermolysis is unaffected (Figure S4.4); thus, the deviation from first-order kinetics at long times is due to some other factors, such as second-order reactions at higher concentrations.

(48) Comparative studies of the rate of thermolysis of **3** were conducted by placing samples side by side in the same bath. The first few data points in the concentration vs time plots often deviated slightly from the first-order kinetics and were omitted. Multiple measurements suggest that these protocols give reproducible rates, within ±10% (Table S3.2).

(49) Lersch, M.; Tilset, M. Mechanistic Aspects of C−H Activation by Pt Complexes. *Chem. Rev.* **2005**, *105*, 2471−2526.

(50) Zhao, S.-B.; Wang, R.-Y.; Wang, S. Intramolecular C−H Activation Directed Self-Assembly of an Organoplatinum(II) Molecular Square. *J. Am. Chem. Soc.* **2007**, *129*, 3092−3093.

(51) Johansson, L.; Tilset, M. Evidence for Associative Methane Loss Following Protonation of (Diimine)$Pt^{II}(CH_3)_2$: Three-Coordinate 14-Electron Cations $L_2Pt(CH_3)^+$ Are Not Necessarily Intermediates in C−H Activation at Cationic Pt Complexes. *J. Am. Chem. Soc.* **2001**, *123*, 739−740.

(52) The measured k_H/k_D values in C_6H_6 are 1.4(2), 1.3(2), and 1.1(2), respectively. The values are the same within error as those in C_6D_6 but have larger errors because the large peak due to the undeuterated solvent interferes with accurate peak integration.

(53) Because the ε (olefinic methylene) protons were monitored during the thermolyses of **3**-γ-d_4 and **3**-δ-d_2, and these protons are slowly deuterated by exchange with one another (by less than 10%, see the Experimental Section), the measured rates for **3**-γ-d_4 and **3**-δ-d_2 are slightly overestimated.

(54) Griffiths, D. C.; Young, G. B. Mechanisms of Thermolytic Rearrangement of Dineophylplatinum(II) Complexes via Intramolecular Carbon-Hydrogen Bond Activation. *Organometallics* **1989**, *8*, 875−886.

(55) Chen, G. S.; Labinger, J. A.; Bercaw, J. E. The Role of Alkane Coordination in C−H bond Cleavage at a Pt(II) Center. *Proc. Natl. Acad. Sci. U. S. A.* **2007**, *104*, 6915.

(56) Johansson, L.; Tilset, M.; Labinger, J. A.; Bercaw, J. E. Mechanistic Investigation of Benzene C−H Activation at a Cationic Platinum(II) Center: Direct Observation of a Platinum(II) Benzene Adduct. *J. Am. Chem. Soc.* **2000**, *122*, 10846−10855.

(57) This result is consistent with previous reports that neopentyl-type alkyl groups are prone to C−H activation at positions δ to platinum. See: DiCosimo, R.; Moore, S. S.; Sowinski, A. F.; Whitesides, G. M. Cyclometalation of Dialkylbis(triethylphosphine)-platinum(II) Complexes: Formation of Pt,Pt-Bis(triethylphosphine)-platinacycloalkanes. *J. Am. Chem. Soc.* **1982**, *104*, 124−133.

(58) The primary KIE for activation of δ-C−H bonds and the absence of scrambling into the α-site confirms the conclusion drawn from the formation of only trivial amounts of methylenecyclobutane (and cyclobutene) products: i.e., that the primary thermolysis pathway does not involve migratory insertion of the olefin into the Pt−alkyl bond (mechanism b, Scheme 1).

(59) Simmons, E. M.; Hartwig, J. F. On the Interpretation of Deuterium Kinetic Isotope Effects in C−H Bond Functionalizations by Transition-Metal Complexes. *Angew. Chem., Int. Ed.* **2012**, *51*, 3066−3072.

(60) Owen, J. S.; Labinger, J. A.; Bercaw, J. E. Kinetics and Mechanism of Methane, Methanol, and Dimethyl Ether C−H Activation with Electrophilic Platinum Complexes. *J. Am. Chem. Soc.* **2006**, *128*, 2005−2016.

(61) Zhong, H. A.; Labinger, J. A.; Bercaw, J. E. C−H Bond Activation by Cationic Platinum(II) Complexes: Ligand Electronic and Steric Effects. *J. Am. Chem. Soc.* **2002**, *124*, 1378−1399.

(62) McKeown, B. A.; Gonzalez, H. E.; Friedfeld, M. R.; Gunnoe, T. B.; Cundari, T. R.; Sabat, M. Mechanistic Studies of Ethylene Hydrophenylation Catalyzed by Bipyridyl Pt(II) Complexes. *J. Am. Chem. Soc.* **2011**, *133*, 19131−19152.

(63) Procelewska, J.; Zahl, A.; van Eldik, R.; Zhong, H. A.; Labinger, J. A.; Bercaw, J. E. Activation Volume Measurement for C−H Activation. Evidence for Associative Benzene Substitution at a Platinum(II) Center. *Inorg. Chem.* **2002**, *41*, 2808−2810.

(64) Clot, E.; Eisenstein, O.; Jasim, N.; Macgregor, S. A.; McGrady, J. E.; Perutz, R. N. C−F and C−H Bond Activation of Fluorobenzenes and Fluoropyridines at Transition Metal Centers: How Fluorine Tips the Scales. *Acc. Chem. Res.* **2011**, *44*, 333−348.

(65) McDermott, J. X.; White, J. F.; Whitesides, G. M. Thermal Decomposition of Bis(phosphine)platinum(II) Metallocycles. *J. Am. Chem. Soc.* **1976**, *98*, 6521−6528.

(66) Tagge, C. D.; Simpson, R. D.; Bergman, R. G.; Hostetler, M. J.; Girolami, G. S.; Nuzzo, R. G. Synthesis of a Novel Volatile Platinum Complex for Use in CVD and a Study of the Mechanism of Its Thermal Decomposition in Solution. *J. Am. Chem. Soc.* **1996**, *118*, 2634−2643.

(67) Wilkinson, G. The Transition Metal to Carbon Sigma Bond. *Pure Appl. Chem.* **1972**, *30*, 627−636.

(68) Collier, M. R.; Lappert, M. F.; Truelock, M. M. μ-Methylene Transition Metal Binuclear Compounds: Complexes with Me_3SiCH_2− and Related Ligands. *J. Organomet. Chem.* **1970**, *25*, C36−C38.

(69) Wilkinson, G. The Long Search for Stable Transition Metal Alkyls. *Science* **1974**, *185*, 109.

(70) Yagupsky, G.; Mowat, W.; Shortland, A.; Wilkinson, G. Trimethylsilylmethyl Compounds of Transition Metals. *J. Chem. Soc. D* **1970**, 1369−1370.

(71) Somorjai, G. A.; Blakely, D. W. Mechanism of Catalysis of Hydrocarbon Reactions by Platinum Surfaces. *Nature* **1975**, *258*, 580−583.

(72) Somorjai, G. A.; Zaera, F. Heterogeneous catalysis on the molecular scale. *J. Phys. Chem.* **1982**, *86*, 3070−3078.

(73) Geyer, S. M.; Methaapanon, R.; Shong, B.; Pianetta, P. A.; Bent, S. F. In Vacuo Photoemission Studies of Platinum Atomic Layer Deposition Using Synchrotron Radiation. *J. Phys. Chem. Lett.* **2013**, *4*, 176−179.

(74) Brunauer, S.; Emmett, P. H.; Teller, E. Adsorption of Gases in Multimolecular Layers. *J. Am. Chem. Soc.* **1938**, *60*, 309−319.

(75) Low, J. J.; Goddard, W. A. Theoretical Studies of Oxidative Addition and Reductive Elimination. 3. Carbon-Hydrogen and Carbon-Carbon Reductive Coupling from Palladium and Platinum Bis(phosphine) Complexes. *J. Am. Chem. Soc.* **1986**, *108*, 6115−6128.

(76) Elam, J. W.; Zinovev, A. V. V.; Pellin, M. J.; Comstock, D. J.; Hersam, M. C. Nucleation and Growth of Noble Metals on Oxide Surfaces Using Atomic Layer Deposition. *ECS Trans.* **2006**, *3*, 271−278.

(77) Cheon, J.; Rogers, D. M.; Girolami, G. S. Mechanistic Studies of the Thermolysis of Tetraneopentyltitanium(IV). 1. Solution Evidence That Titanium Alkylidenes Activate Saturated Hydrocarbons. *J. Am. Chem. Soc.* **1997**, *119*, 6804−6813.

(78) Liu, S.; Gray, D.; Zhu, L.; Girolami, G. S. Lithium−Olefin π-Complexes and the Mechanism of Carbolithiation: Synthesis, Solution Behavior, and Crystal Structure of (2,2-Dimethylpent-4-en-1-yl)lithium. *Organometallics* **2019**, *38*, 2199−2210.

https://dx.doi.org/10.1021/acs.organomet.0c00542
Organometallics 2020, 39, 3817−3829